

# Revisiting the Wu-Yang Monopole: classical solutions and conformal invariance

J. A. O. Marinho\* and O. Oliveira†  
*CFC, Dep Física, Universidade de Coimbra, 3004 516 Coimbra, Portugal*

B. V. Carlson‡ and T. Frederico§  
*Departamento de Física, Instituto Tecnológico de Aeronáutica, 12.228-900, São José dos Campos, SP, Brazil*

The Wu-Yang monopole for pure SU(2) Yang-Mills theory is revisited. New classical solutions with finite energy are found for a generalized Wu-Yang configuration. Our method relies on known asymptotic series solutions and explores the conformal invariance of the theory to set the scale for the monopole configurations. Furthermore, by breaking the scale invariance of the pure Yang-Mills theory by a term which simulates the coupling to quark fields, four different monopole configurations with an energy of 2.9 GeV and spatial extent of 1.2 fm, 1.4 fm, 2.4 fm and 2.6 fm are obtained. These configurations may play a role in the transition to the plasma phase.

PACS numbers: 12.38.Aw, 14.80.Hv, 11.27.+d, 11.15.-q

## I. INTRODUCTON AND MOTIVATION

Classical solutions of Yang-Mills theory can provide new insights into non-perturbative physics, giving hints on infrared properties (related to confinement or chiral symmetry breaking, for example). Among the known classical solutions, we can name several configurations which have been investigated and used in studies of hadronic phenomenology: the instanton, meron, dyon and monopole (for a review, see [1]). Furthermore, in spite of the dyon being a kind of generalized monopole solution [2], and the existence of a possible meron-monopole connection [3], the monopole solution seems to play a special role at the level of the basic structure of the theory. Multipole solutions have also been discussed in the literature [4].

Here we want to revisit the monopole solution, addressing the generalized Wu-Yang monopole (WYM) [5]. The simple WYM is a Dirac magnetic monopole imbedded in the SU(2) gauge group, written in a simple form as:

$$A^{0a} = 0 ; \quad A^{ia} = \epsilon^{iab} \frac{x_b}{r^2} . \quad (1)$$

Among recent uses of the WYM, one could cite that the description of nuclear motion in a diatomic molecule can possess a Wu-Yang like-term [6]. Moreover, the screening effects in non-abelian Quark-Gluon Plasmas may give rise to Wu-Yang terms as well [7]. Furthermore, in [8] the monopole solution is used in the equation for the inverse of the quark propagator. There, a spin-orbit term is computed together with an energy spectrum.

Less recent is the belief that a condensed phase of monopoles could encode the key of the confinement mechanism. Some authors argue that in the maximal abelian

sub-algebra of the Yang-Mills theory, the monopole assumes a crucial role in long distance effects, such that it gives rise to a so-called “Abelian dominance” [9].

The WYM has also been used to investigate Gribov copies [10]. This connects with the problem of building a suitable generating functional for the Yang-Mills theory Green’s functions valid beyond perturbation theory.

In this work, our goal is to obtain solutions of the field equations assuming a WYM configuration. With this in hands, one can estimate an energy scale and study Gribov copies, among other applications.

The classical configurations that we are going to discuss are of the generalized WYM type

$$A^{ia} = \epsilon^{iab} \frac{x_b}{r^2} f(r) . \quad (2)$$

Of course the generalized WYM keeps its primitive nature. It mixes the color and the space indices in the same way, and includes the original WYM as a particular case. The corresponding field equation is a nonlinear ordinary differential equation for  $f(r)$  that will be investigated with a combination of analytical and numerical tools. This paper is organized as follows. In section II, the generalized Wu-Yang configuration is discussed, with the computation of  $F_{\mu\nu}^a$  and the classical energy. In III the solutions of the classical equation of motion as power series is discussed. In section IV two different numerical solutions of the classical field equation are computed and their chromomagnetic fields, for large and small  $r$ , are discussed. In section V we explore the conformal invariance of the theory to introduce a mass scale of the order of a typical nonperturbative scale  $\sim 1$  GeV (or  $\sim 1$  fm) for the monopole. Then, one can estimate the monopole size (energy). Monopole like configurations with discontinuous first derivatives are discussed in VI. Finally, in VII we resume and conclude.

\* adnei@ita.br

† orlando@teor.fis.uc.pt

‡ brett@ita.br

§ tobias@ita.br

## II. GENERALIZED WU-YANG MONOPOLE ANSATZ

In this work, we are going to treat several classical aspects of the Yang-Mills theory, given by the Lagrangian density  $\mathcal{L} = -\frac{1}{4} F_{\mu\nu}^a F_a^{\mu\nu}$ . From now on, it will be assumed that the rescaling of the gauge fields has been performed, so that the coupling constant  $g$  will be omitted. Furthermore, only the SU(2) gauge group will be considered, for the sake of simplicity.

The classical equations of motion are a set of coupled non-linear partial differential equations. Among the possible classical configurations, one may take the generalized Wu-Yang monopole discussed previously. The time component of the gauge field vanishes,  $A_0^a = 0$ , and the spatial components are given by equation (2). Note that this static configuration satisfies the Lorentz,  $\partial^\mu A_\mu^a = 0$ , and Coulomb,  $\nabla \cdot \vec{A}^a = 0$ , gauge fixing conditions automatically.

Here one might of course pose the question of the completeness of this configuration. Indeed, the  $f(r)$  function accounts for distance fluctuations. However, in terms of directions in the color space, one could think that the monopole configuration is very restricted. Further, we see that the mixing of color and space-time indices is also a quite strong restriction.

Let us go ahead and calculate the Lagrangian density. It is just a matter of algebraic work to find the form of the nonabelian gauge tensor due to the generalized Wu-Yang configuration. It reads

$$F_{ij}^a = \left( \frac{f'}{r^3} - 2 \frac{f}{r^4} \right) [x^i \epsilon_{jab} x^b - x^j \epsilon_{iab} x^b] + 2 \frac{f}{r^2} \epsilon_{ija} - \frac{f^2}{r^4} \epsilon_{ijb} x^b x^a, \quad (3)$$

$$F_{0j}^a = 0; \quad (4)$$

Note that the chromoelectric field vanish. Another important object is the energy density, obtained by the contraction of the  $F_{\mu\nu}$  tensor. Then, the corresponding chromomagnetic energy density is

$$\frac{1}{4} (F_{ij}^a)^2 = \left( \frac{f'}{r} \right)^2 + 2 \frac{f^2}{r^4} - 2 \frac{f^3}{r^4} + \frac{1}{2} \frac{f^4}{r^4}. \quad (5)$$

The total energy is given after integrating (5) over the space volume. Now, it is convenient to make the replacement  $f = g + 1$ , which gives the energy as:

$$\mathcal{E} = 4\pi \int_0^{+\infty} dr \left\{ (g')^2 + \frac{(g^2 - 1)^2}{2r^2} \right\}. \quad (6)$$

Of course, depending on the form of the integrand,  $g(r)$  may have a confining shape or not. Note that the requirement of finite energy prevents  $g(r)$  of growing without bound with  $r$ . To achieve the solutions for  $g(r)$ , one has to solve the equations of motion, obtained by requiring

that  $g(r)$  minimizes the energy. The equation of motion reads:

$$g'' = \frac{g}{r^2} (g^2 - 1). \quad (7)$$

This equation, obtained by minimizing the energy, is exactly the same one that is derived using (2) in the classical equations of motion of the classical Yang-Mills theory. Of course, first one has to solve equation (7) to compute the classical energy from the generalized WYM configurations.

## III. SERIES SOLUTION

Given that (7) is nonlinear, it is quite difficult if not impossible to get an analytical solution. Then, let us construct a series to approximate the solution. First note that equation (7) is symmetric under scale transformations: if  $g(r)$  is a solution, then  $g(\lambda r)$  is also a solution, for any  $\lambda > 0$ . To see this, multiply the equation by  $\lambda^2$  and convert it to an identical equation in the new variable  $x = r/\lambda$ , whose solution is  $g(\lambda x)$ . Next, note that any finite solution must remain in the interval  $-1 \leq g(r) \leq 1$ . If  $g(r) > 1$  with  $g'(r) > 0$ , a necessary condition for approaching the value 1 from below, the solution grows without bound. If  $g(r) < -1$  with  $g'(r) < 0$ , a necessary condition for approaching  $-1$  from above, the solution diminishes without bound. Furthermore, for a solution of the equation to be finite in the limits of its domain, we must have

$$g(r) \rightarrow \pm \left( 1 - (\lambda_l r)^2 \right) \quad r \rightarrow 0 \quad (8)$$

and

$$g(r) \rightarrow \pm \left( 1 - \frac{1}{\lambda_h r} \right) \quad r \rightarrow \infty, \quad (9)$$

for some  $\lambda_l$  and  $\lambda_h$ . Further, we note that if  $g(r)$  is a solution, then  $-g(r)$  is as well.

This is sufficient to give us a hint about the necessary form of the required series solution. We cast the solution  $g(r)$  as:

$$g(r) = \begin{cases} A(r) = \sum_{n=0}^{N_A} a_n r^n, & (0 \leq r \leq R) \\ B(r) = \sum_{n=0}^{N_B} b_n r^{-n}, & (R \leq r) \end{cases} \quad (10)$$

The reader should be aware that the first terms of these series are well known - see, for instance, appendix G of [1].

The function  $g(r)$  presents distinct behaviors depending on the distance to the origin. For small  $r$ ,  $A(r)$  favors growth of the interaction with increasing distance. For  $r$  greater than  $R$ ,  $B(r)$  favors the decrease of the interaction with distance.

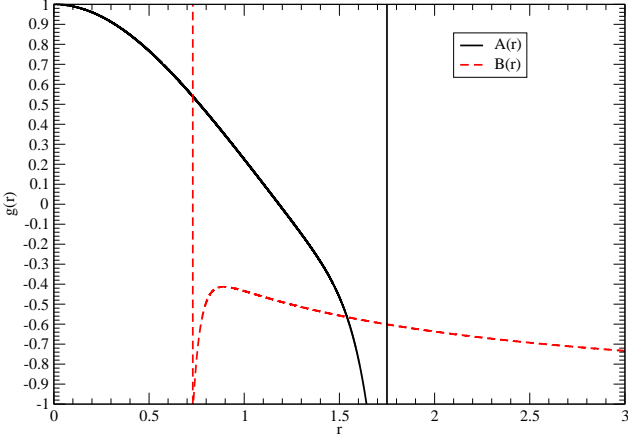


FIG. 1. The series solutions  $A(r)$  and  $B(r)$ . The vertical lines are the naive radius of convergence for each series - see text for details.

Using the above solution in the differential equation (7), a recursion relation for the various  $a_n$  and another for the  $b_n$  coefficients can be derived. Indeed, to lowest order in  $r$  or in  $1/r$  for the  $A(r)$  and  $B(r)$  functions, respectively, one has that  $a_0^3 - a_0 = b_0^3 - b_0 = 0$ . Therefore  $a_0 = 0, \pm 1$  and  $b_0 = 0, \pm 1$ . The zero value implies always the trivial solution, i.e.  $a_n = 0$  and/or  $b_n = 0$ . Given the symmetry  $g(r) \rightarrow -g(r)$ , we will consider only the  $+1$  solution. Furthermore, for  $A(r)$  it turns out that the coefficients for odd powers of  $r$  vanish. After redefining the  $A(r)$  series to include only even powers of  $r$  and using the  $+1$  value for the  $a_0$  and  $b_0$ , the  $a_1$  and  $b_1$  coefficients are arbitrary and the remaining coefficients are given in terms of  $a_1$  and  $b_1$ .

In the following, in the computation of  $A(r)$  and  $B(r)$  the truncations  $N_A = N_B = 18$  are used everywhere. For completeness, we write the first terms of the series solutions. For  $a_1 = b_1 = 1$ , it comes that

$$\begin{aligned} A(r) = 1 - r^2 + \frac{3}{10}r^4 - \frac{1}{10}r^6 + \frac{59}{1800}r^8 - \frac{71}{6600}r^{10} \\ + \frac{15143}{4290000}r^{12} - \frac{20327}{17550000}r^{14} + \frac{1995599}{5250960000}r^{16} \\ - \frac{311031533}{249420600000}r^{18} \end{aligned} \quad (11)$$

and

$$\begin{aligned} B(r) = 1 - \frac{1}{r} + \frac{3}{4}\frac{1}{r^2} - \frac{11}{20}\frac{1}{r^3} + \frac{193}{480}\frac{1}{r^4} - \frac{47}{160}\frac{1}{r^5} \\ + \frac{3433}{16000}\frac{1}{r^6} - \frac{67699}{432000}\frac{1}{r^7} + \frac{1318507}{11520000}\frac{1}{r^8} \\ - \frac{2118509}{25344000}\frac{1}{r^9} \end{aligned} \quad (12)$$

We call the reader attention that, due to conformal invariance,  $A(r)$  and  $A(\lambda r)$  or  $B(r)$  and  $B(\lambda r)$  are solutions of the equations of motion. For the truncation described above, one can estimate the radius of convergence of the series from the higher order terms in the series. For  $A(r)$

convergence occurs for  $r < 1.75$ , while for the  $B(r)$  series convergence happens for  $r > 0.73$ .

We have investigated how the naive estimate of the radius of convergence changes with the order of the truncation, i.e. with  $N_A$  and with  $N_B$ . The analysis of the series for  $A(r)$  and  $B(r)$  show that, with the exception of the first few terms, the estimate of the radius of convergence is almost independent of  $N_A$  and  $N_B$ . We can then consider matching the series  $A(r)$  to the value and first derivative of the series  $B(\lambda r)$  for some  $\lambda$  and some  $r$  in the interval  $0.73/\lambda < r < 1.75$ . It can be shown, however, that such values of  $\lambda$  and  $r$  do not exist, which prevents the construction of a global solution of (7) in the form of the power series.

The series solutions can be seen in figure 1 together with the naive radius of convergence.

#### IV. NUMERICAL SOLUTIONS

A numerical solution of equation (7) can be built combining the series for  $A(r)$  and  $B(r)$ , described in the previous section, with a Taylor expansion of  $g(r)$ . If at  $r = r_0$  the solution  $g(r)$  along with its first and second derivatives are known, one can expand  $g(r)$  around  $r_0$

$$g(r_0 + \delta r) = g(r_0) + g'(r_0)\delta r + \frac{1}{2}g''(r_0)(\delta r)^2 + \dots \quad (13)$$

and similar expansions for  $g'(r)$  and  $g''(r)$  can be written. Replacing, in the differential equation (7), the expansion for  $g(r_0 + \delta r)$  and  $g''(r_0 + \delta r)$ , working order by order in  $\delta r$ , one can compute the derivatives  $g^{(n)}(r_0)$  for  $n = 3, 4, \dots$  in terms of  $g(r_0)$ ,  $g'(r_0)$  and  $g''(r_0)$ . In our numerical solutions, discussed below, we have considered expansions of  $g(r)$  up to order 6.

For the solution called  $g_{int}(r)$ , the integration starts at  $r = 0$ , setting  $g(r) = A(r)$ , and using an integration step of  $\delta r = 10^{-4}$ . The series solution was used up to the point where the relative error between the l.h.s. and r.h.s. of equation (7) was below a certain error, which we took to be  $10^{-6}$ . If the solution  $g \sim 0$ , then instead of the relative error we have used the absolute error, i.e. the absolute difference between the l.h.s. and r.h.s. of the differential equation. This procedure (so far, using  $A(r)$ ) gives  $g(r)$ ,  $g'(r)$  and  $g''(r)$ , as the series for  $A(r)$  up to  $r = 0.61$ . From this point onwards,  $g(r)$  was propagated using the Taylor series procedure described at the beginning of this section. At each step the relative error, or the absolute error, in the differential equation was checked. If the precision was above the tolerance demanded, then the propagation was restarted using the last point where the differential equation was satisfied to calculate the coefficients of the Taylor expansion. The procedure was repeated up to the point where  $|g(r)| = 1$ . From this point onwards it was assumed that  $g(r) = \pm 1$  for all  $r$ , with the sign chosen to produce a continuous function.

For the solution called  $g_{ext}(r)$ , integration was started at  $r = 300$ , setting  $g(r) = -B(r)$ , and using  $\delta r = -10^{-4}$

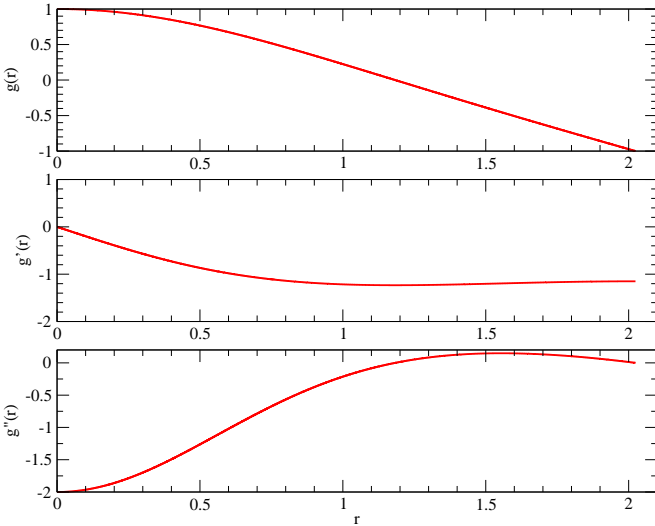


FIG. 2. The solution  $g_{int}(r)$  and its derivatives.

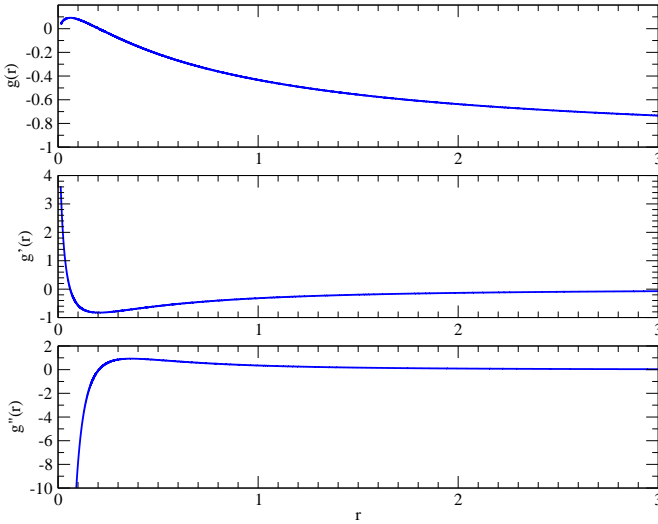


FIG. 3. The solution  $g_{ext}(r)$  and its derivatives.

as integration step. The procedure to compute  $g_{ext}(r)$  follows the same lines as the computation of  $g_{int}(r)$ , with the difference that the solution is now propagated backwards. Deviations from the  $B(r)$  series solution happen for  $r \leq 2.12$ .

The numerical integration was checked exploring different integration steps and the conformal invariance of equation (7). In particular, the scaling of  $g'(r)$  and  $g''(r)$  under a scale transformation was checked carefully. Furthermore, relaxing the precision on the differential equation, we observed that the numerical solution follow the series solution almost up to its naive convergence radius. The several tests performed gave us confidence on our numerics.

The curves for  $g_{int}(r)$  and  $g_{ext}(r)$ , including its first and second derivatives, are shown in figures 2 and 3, re-

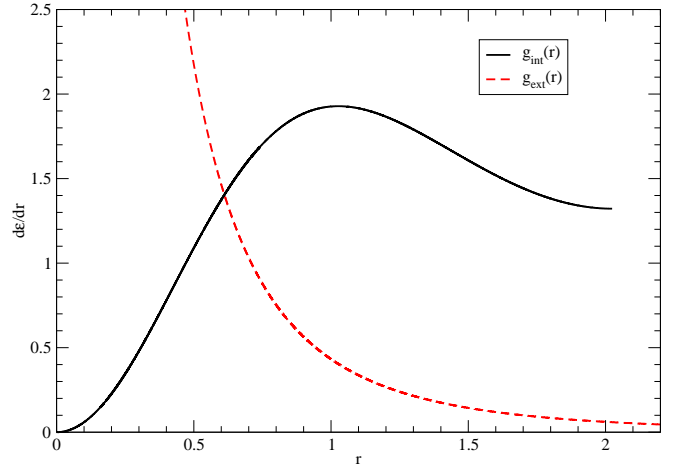


FIG. 4. The energy density for  $g_{int}(r)$  and  $g_{ext}(r)$ .

spectively.

Let us discuss first the solution  $g_{ext}(r)$ .  $g_{ext}(r)$  is the numerical solution found by Wu and Yang in [5]. Although in figure 3, it seems that the curve touches  $r = 0$ , this is not the case. A closer look shows that the smallest value of  $r$  numerically available is 0.0133. Our numerical procedure was not able to go below this value of  $r$ . Anyway  $g_{ext}(r)$  matches perfectly the solution of the linearized field equation (7), i.e.

$$g(r) = \sqrt{r} \left( G_0 \sin \left( \frac{\sqrt{3}}{2} \ln r \right) + G_1 \cos \left( \frac{\sqrt{3}}{2} \ln r \right) \right), \quad (14)$$

with  $G_0 = -0.079223$  and  $G_1 = -0.4251983$ .  $g_{ext}(r)$  oscillates as  $r$  approaches zero and its derivative diverges at  $r = 0$ . The classical energy, as given by (6), associated with  $g_{ext}(r)$  is infinite.

On the other hand, the solution  $g_{int}(r)$  has finite energy,  $\mathcal{E} = 33.63$  in dimensionless units, but its first derivative is discontinuous at  $r = 2.024$  where  $g = -1$ . For  $r > 2.024$  one assumes a constant solution with  $g = -1$  and for  $r > 2.024$  the energy density associated with  $g_{int}(r)$  vanishes. The energy density for  $g_{int}(r)$  and  $g_{ext}(r)$  is reported in figure 4.

### A. The Chromomagnetic Field

The chromomagnetic fields are given in terms of  $f = 1+g$  by equation (3). For each of the numerical solutions described previously, one can build two different  $f = 1 \pm g$  and its large distance behavior is given by

$$g_{int}(r) = -1 \quad \text{and} \quad g_{ext}(r) = 1 - \frac{1}{r}, \quad (15)$$

i.e.

$$f(r) = \begin{cases} 0, & g = +g_{int} \\ 2, & g = -g_{int} \end{cases} \quad (16)$$

and

$$f(r) = \begin{cases} 2 - \frac{1}{r}, & g = +g_{ext} \\ \frac{1}{r}, & g = -g_{ext} \end{cases} \quad (17)$$

For the first solution  $F_{ij}^a = 0$ . For the second and third solutions,  $F_{ij}^a \sim 4/r^2$  at large  $r$ . Finally, for the last solution the chromomagnetic field associated with monopole vanishes faster and goes like  $F_{ij}^a \sim 1/r^3$  at large distances. Given the behavior of  $F_{ij}^a$  at large distance, one can say that solutions two and three are monopole like solutions, i.e.  $F_{ij}^a \sim 1/r^2$ , while the fourth solution is a dipole like solution, i.e.  $F_{ij}^a \sim 1/r^3$ .

In what concerns the short distance behavior, for all configurations  $F_{ij}^a$  diverges at  $r = 0$ . The exception being the trivial solution with a vanishing chromomagnetic field.

## V. WU-YANG MONOPOLES AND CLASSICAL ENERGY

In the previous section we have computed monopole configurations with infinite classical energy (those associated with  $g_{ext}(r)$ ), and monopoles with finite energy (associated with  $g_{int}(r)$ ). However, in what concern monopoles with finite energy, besides the solutions associated with  $g_{int}(r)$ , the constant solutions of the equation of motion (7) also belong to this family of functions. The equation of motion (7) has the constant solutions  $g = 0, \pm 1$  but only  $g = 1$  and  $g = -1$  have finite zero energy - see the definition (6). In particular,  $g = -1$  is associated with the trivial  $A_\mu^a = 0$  configuration and will not be considered any further.

The monopole with  $g = 0$ , i.e.  $f = 1$ , despite having infinite classical energy, has an associated chromomagnetic field vanishing as  $1/r^2$  for large  $r$ .

For the monopole configurations with classical infinite energy, the divergence in  $\mathcal{E}$  is associated with an ultraviolet, i.e. short distance, divergence of the energy density. Like in classical electrodynamics, one can cure the divergence via the introduction of a short distance cutoff. Then, a scale is introduced into the theory and conformal invariance is broken explicitly.

On the other hand, finite energy monopoles are either constant solutions of (7) or have a discontinuity on the first derivative of  $f$ .

Let us go back to the solution  $g_{int}(r)$ . Conformal invariance means that if  $g_{int}(r)$  is a solution of equation (7),  $g_{int}(\lambda r)$  is also a solution of the same differential equation with energy  $33.63/\lambda$ . Assuming that this energy is a typical hadronic scale  $\sim 1$  GeV, then  $\lambda = 33.63 \text{ GeV}^{-1}$  and the discontinuity occurs for  $r_d = 2.024 \lambda = 13.4 \text{ fm}$ , roughly one order of magnitude larger than the typical hadronic scale  $\sim 1 \text{ fm}$ . If instead, one uses the mass of the lowest glueball to set the scale  $M_{glue} = 1.7 \text{ GeV}$  [12], these figures should be divided by 1.7, i.e.  $\lambda = 19.78 \text{ GeV}^{-1}$  and  $r_d = 7.9 \text{ fm}$ . Again, the discontinuity on

the first derivative of  $f$  happens at a rather large length scale.

The hadronic length scale  $\sim 1 \text{ fm}$  comes from the analysis of baryons and mesons constituted by quarks. Our reasoning shows that if the finite energy solution built from  $g_{int}(r)$  plays a role on the dynamics of the Yang-Mills theory, then the large distance behavior is clearly dominated by gluon fields. Furthermore, these gluon fields have a spatial size about ten times larger than the usual quark content. Ignoring, for the moment, possible implications of such a picture on quark matter phenomenology, in the next section we investigate how far can one take the discontinuous monopole configurations.

## VI. DISCONTINUOUS WU-YANG MONOPOLES WITH FINITE ENERGY

Discontinuities in the derivative can be introduced in the field equation (7) via a Dirac-delta function  $\delta(r - R_0)$ . Away from  $r = R_0$  one recovers the original equation and  $g(r)$  is given by one of the solutions discussed in section II. Adding a term like  $\zeta \delta(r - R_0)$ , where  $\zeta$  is a constant, to (7) is equivalent to add  $\zeta g(r) \delta(r - R_0)$  to the density of energy. Remember that the field equation was obtained directly from the classical Yang-Mills equations for the generalized Wu-Yang configuration and from minimizing the energy (6). Such a term can be due to the presence of static quarks located at  $R_0$ . In this sense one can see  $\zeta$  as the square of the quark wave function at  $R_0$  and  $R_0$  as a mean value of the quark radius. Furthermore, the introduction of the new term in  $\mathcal{E}$  for a fixed  $R_0$  breaks conformal invariance.

A physical scale should be introduced in QCD in order to construct the observables. In hadronic physics this is set by  $\Lambda_{\text{QCD}} \sim 1 \text{ fm}^{-1}$ , i.e., the scale where conformal invariance is broken, as in modern bottom-up approaches of the hadronic spectrum within gauge/gravity duality (see e.g. [11]). However, our classical solutions, as we will see, attain too large energies, in the hadronic scale, when the typical extension of the chromagnetic field is of the order of 1 fm, which suggests that it is required a collective phenomena to excite such field configurations. More on that discussion will come later on.

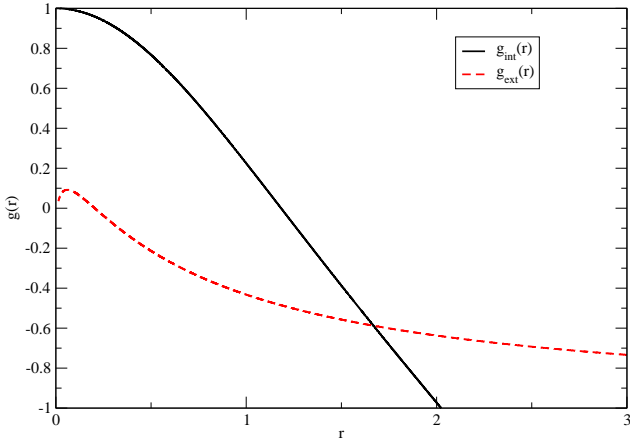
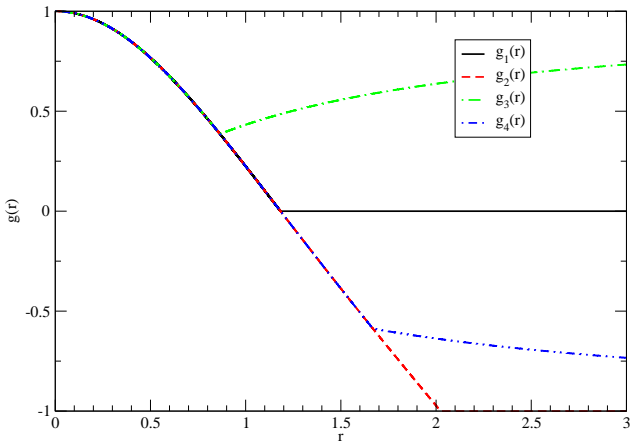
So let us assume that the classical field equation is given by

$$g'' = \frac{g}{r^2} (g^2 - 1) + \zeta \delta(r - R_0). \quad (18)$$

For  $r \neq R_0$  the solutions of (18) are the functions  $g(r)$  discussed in section II - see figure 5. Assuming that  $g(r)$  is continuous at  $R_0$ , integrating (18) from  $R_0 - \epsilon$  to  $R_0 + \epsilon$  gives, in the limit where  $\epsilon \rightarrow 0^+$ ,

$$g'(R_0 + \epsilon) - g'(R_0 - \epsilon) = \zeta. \quad (19)$$

Finite energy solutions require  $g(0) = \pm 1$ . Therefore, for  $r < R_0$  only  $\pm g_{int}(r)$  and the constant solutions  $g = \pm 1$  are acceptable. On the other side, for  $r > R_0$ , there

FIG. 5. The solutions  $g_{int}(r)$  and  $g_{ext}(r)$ .FIG. 6. The solutions  $g_1(r)$  to  $g_4(r)$ .

is no reason to exclude any of the solutions  $\pm g_{int}(r)$ ,  $\pm g_{ext}(r)$ ,  $g(r) = 0$  or  $g(r) = \pm 1$  which can be combined to produce several finite energy solutions. The solution of equation (18) gives an  $f$  continuous and  $f'$  discontinuous at  $R_0$  – see equation (19). The various solutions are

$$g_1(r) = \begin{cases} g_{int}(r) & r \leq R_0 = 1.1831 \\ 0 & r > R_0 \end{cases} \quad (20)$$

for a  $\zeta_1 = 1.2327$ ,

$$g_2(r) = \begin{cases} g_{int}(r) & r \leq R_0 = 2.0240 \\ -1 & r > R_0 \end{cases} \quad (21)$$

with a  $\zeta_3 = 1.1498$ ,

$$g_3(r) = \begin{cases} g_{int}(r) & r \leq R_0 = 0.8651 \\ -g_{ext}(r) & r > R_0 \end{cases} \quad (22)$$

with a  $\zeta_3 = 1.5432$  and

$$g_4(r) = \begin{cases} g_{int}(r) & r \leq R_0 = 1.6685 \\ g_{ext}(r) & r > R_0 \end{cases} \quad (23)$$

with  $\zeta_2 = 1.009$ . In all cases  $\zeta$  was computed with equation (19). The various solutions can be seen in figure 6.

Assuming that the energy density is modified by the term  $\zeta g(r) \delta(r - R_0)$ , then the total energy is given by

$$\mathcal{E} = 4\pi \left( \int_0^{+\infty} dr \left\{ (g')^2 + \frac{(g^2 - 1)^2}{2r^2} \right\} + \zeta g(R_0) \right). \quad (24)$$

Since  $g_1(R_0) = 0$ ,  $g_2(R_0) = -1$ ,  $g_3(R_0) = 0.3859$  and  $g_4(R_0) = -0.5877$ , the energy of the monopoles is, in dimensionless units,  $\tilde{\mathcal{E}}_1 = 17.28$ ,  $\tilde{\mathcal{E}}_2 = 19.18$ ,  $\tilde{\mathcal{E}}_3 = 20.90$ ,  $\tilde{\mathcal{E}}_4 = 21.06$ , respectively. In physical units  $r = \lambda \tilde{r}$ ,  $\mathcal{E} = \tilde{\mathcal{E}}/\lambda$ , where the quantities with tilde are dimensionless. Setting the energy of the monopole to 1 GeV, then  $\lambda_1 = 17.28 \text{ GeV}^{-1} = 3.410 \text{ fm}$ ,  $\lambda_2 = 19.18 \text{ GeV}^{-1} = 3.785 \text{ fm}$ ,  $\lambda_3 = 20.90 \text{ GeV}^{-1} = 4.124 \text{ fm}$ ,  $\lambda_4 = 21.06 \text{ GeV}^{-1} = 4.156 \text{ fm}$ .

In physical units, the discontinuity in the derivative happens at  $\lambda R_0$ . For  $g_1(r)$ , this means 4.0 fm. For  $g_2(r)$  one gets  $\lambda R_0 = 7.7 \text{ fm}$ . For  $g_3(r)$  one gets  $\lambda R_0 = 3.6 \text{ fm}$  and for  $g_4(r)$  it follows that  $\lambda R_0 = 6.9 \text{ fm}$ . Note that if one uses the lowest glueball mass 1.7 GeV [12] to set the scale, one should divide these figures by 1.7, i.e. the discontinuities in the derivative would occur at 2.4 fm, 4.5 fm, 2.1 fm, 4.1 fm for  $g_1(r)$ ,  $g_2(r)$ ,  $g_3(r)$ ,  $g_4(r)$ , respectively, beyond which the chromomagnetic fields would decay, at least, as  $1/r^2$ . Again, the scale at which  $r_d = R_0$  happens is larger, at least two times, than the typical hadronic scale.

In dimensionless units, the energy density for the various solutions under discussion is reported in figure 7. Another measure of the monopole size is given by the maximum in the energy density. For  $g_1(r)$ ,  $g_2(r)$  and  $g_4(r)$  the maximum occur at  $r = 1$ . For  $g_3(r)$  the maximum occur at  $r = 0.8651$ . Given the  $\lambda$  values computed in the previous paragraph, if one assumes a scale of 1 GeV, then the monopole sizes are 3.4 fm, 4.5 fm, 3.6 fm and 4.2 fm for  $g_1(r)$ ,  $g_2(r)$ ,  $g_3(r)$  and  $g_4(r)$ , respectively. Otherwise if one uses the glueball mass to set the scale, the characteristic sizes are 2.0 fm, 2.2 fm, 2.1 fm and 2.4 fm, respectively.

## VII. RESULTS AND DISCUSSION

In this work we have revisited the Wu-Yang monopole for pure SU(2) Yang-Mills theory. Assuming that the function  $f(r) = 1 + g(r)$  in equation (2) can be written as a power series defines, together with the requirement of finite energy, the boundary conditions at infinity and at  $r = 0$ , namely:  $g(0) = \pm 1$  and  $g(\infty) = \pm 1$ . Besides

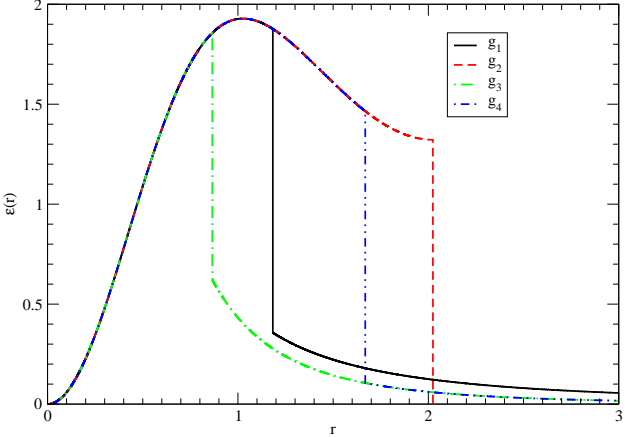


FIG. 7. Energy density, in dimensionless units, for the finite energy solutions  $g_1(r)$ ,  $g_2(r)$  and  $g_3(r)$ . Note the  $1/r^2$  dependence at large  $r$  for  $g_1(r)$ ,  $g_3(r)$  and  $g_4(r)$ .

the constant solutions  $g(r) = 0$  and  $g(r) = 1$ , Wu and Yang were able to find, long ago, a numerical solution with  $g(0) = 0$  and  $g(\infty) = -1$ .

In order to solve the classical equations of motion, we rederived the asymptotic series solutions, close to  $r = 0$ , named  $A(r)$ , and for large  $r$ , named  $B(r)$ . The first terms of the series solutions are given in equations (11) and (12), respectively. We have investigated the two series and tried to build a solution of the equation of motion matching  $A(r)$  up to order  $r^{18}$  and  $B(r)$  up to order  $1/r^{18}$ . It turns out that the radius of convergence make such a type of solution impossible. Indeed, we found that increasing the order of the expansions leaves almost unchanged the naive radius of convergence discussed at the end of section III.

In section IV numerical solutions of the equations of motion were computed and the behavior of their chromomagnetic fields discussed at small and large distances. Our numerical procedure found two different solutions. The numerical solution with  $g(0) = 0$  and  $g(\infty) = -1$  discovered by Wu-Yang, which we named  $g_{ext}(r)$ , and a new solution  $g_{int}(r)$ .

In what concerns  $g_{ext}(r)$ , we were able to provide an analytical description of its behavior at small distances in (14). Further, the classical energy associated with  $g_{ext}(r)$  diverges due to its behavior at  $r \sim 0$ . On the other hand, the energy associated with  $g_{int}(r)$  is finite but one is forced to introduce a discontinuity on the first derivative of  $f(r)$ . Anyway, we have explored the conformal invariance of the theory to set a scale for  $g_{int}(r)$  assuming that its classical energy is a typical hadronic scale. It turns out that the discontinuity, assumed to give a measure of the monopole size, should happen at a length scale which is, at least, four times larger than the typical hadron size. Of course, if one requires that the discontinuity reproduces the typical hadronic size, then is the monopole energy which is to large, at least by a factor of 8, than a typical hadronic mass. However, if

one uses the maximum of the energy density to define the monopole spatial extent, we get a size of  $\sim 6.6$  fm or  $\sim 3.9$  fm assuming a classical energy of 1 GeV or 1.7 GeV, respectively, for the monopole.

In section VI we explore solutions of the classical equation of motion which allow for discontinuities on the first derivative. In particular, a Dirac delta function is added to equation (7). As discussed, such a contribution can be motivated by the presence of quarks. The introduction of a Dirac delta function  $\delta(r - R_0)$  with a fixed  $R_0$ , breaks explicitly invariance of the equations of motion under a scale transformation. Three different discontinuous monopoles configurations (20) - (22) were computed. If one uses a typical hadronic scale to define the monopole energy, then, depending on the scale,  $R_0 = 7.7$  fm or  $R_0 = 2.4$  fm or larger. Again, this is quite a large length scale. Probably, this means that the monopole configurations computed here play a minor role, if any, on low energy phenomenology.

Curiously, if one takes the critical energy density  $\epsilon_c = 0.7$  GeV/fm<sup>3</sup> for the transition to the plasma phase [13] to set the scale, i.e. one puts  $\epsilon_c = (\tilde{\mathcal{E}}/\lambda)/(4\pi R^3/3)$ , where  $\tilde{\mathcal{E}}$  is the dimensionless monopole energy, and take  $R = 1$  fm, a typical hadronic length, then one gets a monopole energy of 2.9 GeV. Using again the discontinuity on the first derivative as a measure of the monopole size, it follows that for the solution  $g_{int}(r)$ , described in section IV,  $\lambda = 2.26$  fm and  $R_0 = 4.6$  fm. Remember that in section IV,  $R_0$  was estimated to be 13.4 fm or 7.9 fm, depending on the choice of scale. For the solution  $g_1(r)$  of section VI,  $\lambda = 1.16$  fm and  $R_0 = 1.38$  fm, to be compared with 4.0 fm or 2.4 fm found in section VI. For the solution  $g_2(r)$ ,  $\lambda = 1.29$  fm and  $R_0 = 2.6$  fm, to be compared with 7.7 fm or 4.5 fm found in section VI. For the solution  $g_3(r)$ ,  $\lambda = 1.41$  fm and  $R_0 = 1.2$  fm, to be compared with 3.6 fm or 2.1 fm found in section VI. For the solution  $g_4(r)$ ,  $\lambda = 1.42$  fm and  $R_0 = 2.4$  fm, to be compared with 6.9 fm or 4.1 fm found in section VI. This suggests that these configurations may play an important role in the confining region and in the transition to the plasma phase. Furthermore, the so-called discontinuous solutions, with sizes in the range 1.2 – 2.6 fm, are considerable shorter than  $g_{int}(r)$ . The difference is certainly due to the Dirac-delta term introduced in the equation and can be seen as a clear sign of the role of the breaking of conformal invariance due to the coupling to the quark fields. Hopefully, one would be able to investigate possible signatures for identifying the monopole configurations in the transition to the plasma phase, in ongoing and future experiments to probe this state of matter with high-energy heavy ion collisions.

## ACKNOWLEDGMENTS

This work was partially supported by Capes/FCT project 183/07. TF and BVC acknowledge partial financial support from FAPESP and CNPq. JAOM ac-

knowledges financial support from CAPES under con-

tract number BEX4092/08-2.

---

- [1] A. Actor, Rev. Mod. Phys. **51**, 461-525 (1979).
- [2] B. Julia, A. Zee, Phys. Rev. **D11**, 2227-2232 (1975).
- [3] A. Actor, Z.Phys. **C6**, 223-234 (1980).
- [4] See, for example, A. D. Popov, J. Math. Phys. **46**, 073506 (2005) and references their in.
- [5] T.T. Wu, C.N. Yang, in *Properties of Matter Under Unusual Conditions*, edited by H. Mark and S. Fernbach (Interscience, New York, 1968).
- [6] J. Moody, A. Shapere, F. Wilczek, Phys. Rev. Lett. **56**, 893 (1986).
- [7] J.-P. Blaizot, E. Iancu, Phys. Rep. **359**, 355-528 (2001).
- [8] R. L. Stuller, Phys. Rev. **D22**, 2510 (1980).
- [9] Z.F. Ezawa, A. Iwazaki, Phys.Rev. **D25**, 2681 (1982).
- [10] B. Holdom, Phys. Rev. **D79**, 085013 (2009).
- [11] G. F. de Teramond, S. J. Brodsky, Phys. Rev. Lett. **102**, 081601 (2009); and references therein.
- [12] Y. Chen et al, Phys.Rev. **D73**, 014516 (2006).
- [13] F.Karsch, E.Laermann, [hep-lat/0305025](https://arxiv.org/abs/hep-lat/0305025).